Circumstantial Evidence for Critical Behavior in Peripheral Au + Au Collisions at 35 MeV/nucleon

P. F. Mastinu,[1] M. Belkacem,[1,9] M. D'Agostino,[1] M. Bruno,[1] P. M. Milazzo,[1,2] G. Vannini,[2] D. R. Bowman,[7] N. Colonna,[3] J. D. Dinius,[6] A. Ferrero,[4,8] M. L. Fiandri,[1] C. K. Gelbke,[6] T. Glasmacher,[6] F. Gramegna,[5] D. O. Handzy,[6] D. Horn,[7] W. C. Hsi,[6] M. Huang,[6] I. Iori,[4] G. J. Kunde,[6] M. A. Lisa,[6] W. G. Lynch,[6] G. V. Margagliotti,[2] C. P. Montoya,[6] A. Moroni,[4] G. F. Peaslee,[6] F. Petruzzelli,[4] R. Rui,[2] C. Schwarz,[6] M. B. Tsang,[6] C. Williams,[6] V. Latora,[9] and A. Bonasera[9]

(Multics-Miniball Collaboration)

[1]*Dipartimento di Fisica and Istituto Nazionale di Fisica Nucleare, Bologna, Italy*
[2]*Dipartimento di Fisica and Istituto Nazionale di Fisica Nucleare, Trieste, Italy*
[3]*Istituto Nazionale di Fisica Nucleare, Bari, Italy*
[4]*Dipartimento di Fisica and Istituto Nazionale di Fisica Nucleare, Milano, Italy*
[5]*Istituto Nazionale di Fisica Nucleare, Laboratori Nazionali di Legnaro, Italy*
[6]*National Superconducting Cyclotron Laboratory, Michigan State University, East Lansing, Michigan 48824*
[7]*Chalk River Laboratories, Chalk River, Canada*
[8]*Comisión Nacional de Energía Atomica, Buenos Aires, Argentina*
[9]*Istituto Nazionale di Fisica Nucleare, Laboratorio Nazionale del Sud, Catania, Italy*

(Received 1 December 1995)

The fragmentation resulting from peripheral Au + Au collisions at an incident energy of $E = 35$ MeV/nucleon is investigated. A power-law charge distribution, $A^{-\tau}$ with $\tau \approx 2.2$, and an intermittency signal are observed for events selected in the region of the Campi scatter plot where "critical" behavior is expected.

PACS numbers: 25.70.Pq, 05.70.Jk, 24.60.Ky

Initiated by the observation of fragments in the final stages of the reaction exhibiting a power law in fragment charge distributions [1], and stimulated by the similarity of the nuclear matter equation of state with that of a van der Waals gas [2], the possibility of observing a liquid-gas phase transition in nuclear systems has been the subject of intensive investigations [3–7]. This interest increased recently with attempts of extracting critical exponents of fragmenting nuclear systems produced in Au + C collisions at $E = 1$ GeV/nucleon [5] and a "caloric curve" for projectile fragmentation reactions in Au + Au collisions at 600 MeV/nucleon [7]. In this Letter, we report results obtained for peripheral Au + Au collisions at $E = 35$ MeV/nucleon which display some characteristics similar to those predicted for near-critical systems.

The experiment was performed at the National Superconducting Cyclotron Laboratory of the Michigan State University. Fragments with charge up to $Z = 83$ were detected at $3° \leq \theta_{\mathrm{lab}} < 23°$ by the Multics array [8], and charged particles with charge up to $Z = 20$ were detected at $23° \leq \theta_{\mathrm{lab}} \leq 160°$ by 159 phoswich detector elements of the MSU Miniball [9]. The charge identification thresholds were about 1.5 MeV/nucleon in the Multics array, independently of the fragment charge, and about 2, 3, 4 MeV/nucleon in the Miniball for $Z = 3$, 10, 18, respectively. The geometric acceptance of the combined apparatuses was greater than 87% of 4π.

Our analysis is guided by calculations [6,10,11] which predict that the "critical" excitation energy may decrease when the system is either charged and/or rotating. Short-lived systems formed in central Au + Au collisions are predicted to expand and undergo a multifragment breakup due to the high combined charge of projectile and target nuclei. Evidence for such Coulomb-driven breakup of a single source has, indeed, been observed [12] in central collisions for this reaction. For larger impact parameters, however, several smaller sources can emerge corresponding to the decay of projectile and targetlike residues and a "neck" [13] that momentarily joins them. With an appropriate reaction filter, one might then hope to select primary fragments with excitation energies, Coulomb charges, and angular momenta appropriate to bring the system into different portions of the instability region [10,14].

Studies with the classical molecular dynamics (CMD) model indicated that critical behavior may be achieved for peripheral Au + Au collisions at $E = 35$ MeV/nucleon [15]. When these CMD results are filtered by the acceptance of the Multics-Miniball arrays, the signals which may be indicative of criticality become washed out due to poorly detected events, but they can be recovered by restricting the analysis to more completely detected peripheral events for which the largest projectilelike fragment (PLF) is detected. Guided by these calculations, we select events for which the largest fragment has a velocity along the beam axis larger than 75% of the beam velocity and the total detected charge is between 70 and 90. For these events, the total detected linear momentum is larger than 50% of the beam momentum. Their distribution of

 0031-9007/96/76(15)/2646(4)$10.00 © 1996 The American Physical Society

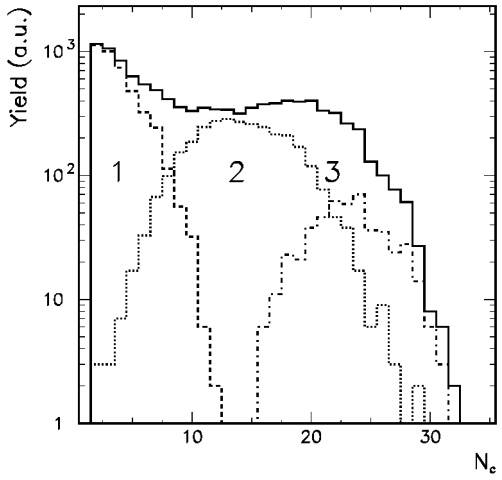

FIG. 1. Multiplicity distribution of the events selected for the analysis (solid histogram). The three dashed histograms (1, 2, and 3) represent the multiplicity distributions of the events falling in the three cuts drawn in Fig. 2.

charged particle multiplicities, N_c, is shown by the solid histogram in Fig. 1.

Figure 2 shows a scatter plot of $\ln(Z^j_{\max})$ versus $\ln(M^j_2)$ ("Campi scatter plot" [16]) where $Z^j_{\max}$ is the charge of the heaviest fragment and M^j_2 is the second conditional moment of the charge distribution detected in the jth event,

$$M_2^{(j)} = \sum_Z Z^2 n_j(Z) . \qquad (1)$$

Here, $n_j(Z)$ denotes the number of fragments of charge Z detected in the jth event, and the summation is over all fragments but the heaviest detected one. Theoretical investigations suggest that such plots may be useful in characterizing near-critical behavior of finite systems [16]. The calculated Campi scatter plots typically exhibit two branches: an upper branch with a negative slope containing

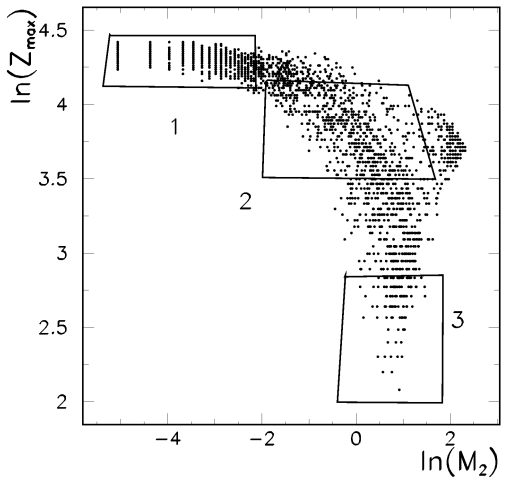

FIG. 2. Campi scatter plot, $\ln(Z_{\max})$ vs $\ln(M_2)$. The three different regions are discussed in the text. Fission events are to the right of region 2.

largely undercritical events (e.g., $T < T_{\rm crit}$ in a liquid-gas phase transition or $p > p_{\rm crit}$ in a percolation phase transition) and a lower branch with a positive slope containing largely overcritical events ($T > T_{\rm crit}$ or $p < p_{\rm crit}$). The two branches were shown to meet close to the critical point of the phase transition [6,16,17].

The data shown in Fig. 2 display two branches similar to the ones predicted for undercritical and overcritical events. In the top-right part, close to the intersection of these two branches (potentially containing near-critical events), a separate island is observed which is due to fission events, as first noted by Ref. [17]. By appropriate gates in the Campi plot, these fission events are removed from the following analysis.

To further investigate the two branches observed in Fig. 2 and the region where they intersect, we employ three cuts selecting the upper branch (cut 1), the lower branch (cut 3), and the intersection region (cut 2); these cuts are indicated in Fig. 2. The charged particle multiplicity distributions observed for these three cuts are shown as dashed histograms in Fig. 1. Cuts 1 and 3 largely select low and high multiplicity events corresponding to very peripheral and central collisions (assuming on the average a monotonic relation between N_c and impact parameter); cut 2 represents a wide range of charged particle multiplicities and thus may involve a wide range of intermediate impact parameters. Thus emission from a unique source cannot be ascertained for cut 2, and it is likely that this cut contains contributions from projectile and targetlike sources and from the neck [13] which emits lighter fragments ($Z \approx 6$–9) with enhanced probability as compared to the projectile residue [13]. However, one does not exclude that this large multiplicity distribution is related to the occurrence of large fluctuations as expected at the critical point.

Fragment charge distributions, not corrected for detection efficiency, are presented [18] for the three cuts in Fig. 3. Cut 1 (crosses) contains both light fragments and heavy residues and thus resembles the "U"-shaped distributions predicted by percolation calculations in the subcritical region [19]. For cut 3 (open circles), one observes an unusually flat charge distribution similar to the one previously reported [12] for central collisions which were selected without the specific constraints employed in this paper and attributed to a Coulomb-driven breakup of a very heavy composite system [12]. (The steep falloff at large Z is an artifact of the selection of events with $Z = 70$–90 used in this paper.) For cut 2 (solid points), a fragment charge distribution is observed which resembles a power-law distribution, $P(Z) \propto Z^{-\tau}$, with $\tau \approx 2.2$. For macroscopic systems exhibiting a liquid-gas phase transition, such a power-law distribution is predicted to occur near the critical point [20]. However, it is not yet known by how much the final fragment distributions differ from the primary ones after the sequential decays of particle unstable primary fragments.

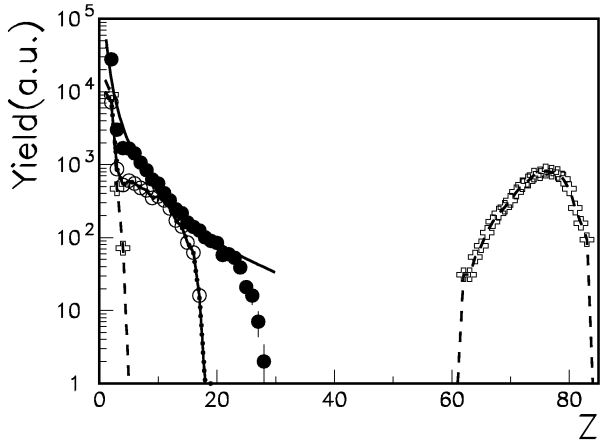

FIG. 3. Charge distributions for the three cuts indicated in Fig. 2. The curve represents a power-law distribution $Z^{-\tau}$ with $\tau \approx 2.2$.

Figure 4 shows [18] the logarithm of the scaled factorial moments (SFM), defined as

$$F_i(\delta s) = \frac{\sum_{k=1}^{Z_{\rm tot}/\delta s} \langle n_k \times (n_k - 1) \times \cdots \times (n_k - i + 1) \rangle}{\sum_{k=1}^{Z_{\rm tot}/\delta s} \langle n_k \rangle^i} \tag{2}$$

($i = 2, \ldots, 5$), as a function of the logarithm of the bin size δs. In the above definition of the SFM, $Z_{\rm tot} = 158$ and i is the order of the moment. The total interval $[1, Z_{\rm tot}]$ is divided into $M = Z_{\rm tot}/\delta s$ bins of size δs, n_k is the number of particles in the kth bin for an event, and the brackets denote the average over many events. A linear rise of the logarithm of the SFM versus δs (i.e., $F_i \propto \delta s^{-\lambda_i}$) indicates an intermittent pattern of fluctuations [17,21,22]. Even though this quantity is ill defined for fragment distributions [23–25], several theoretical studies have indicated that critical events give a power law for the SFM versus the bin size [6,22]. For cut 3 (right part of the figure), the logarithm of the scaled factorial moments $\ln(F_i)$ is always negative (i.e., the variances are smaller than Poissonian [22]) and almost independent on δs; there is no intermittency signal. The situation is different for cut 2 (central part). The logarithm of the scaled factorial moments is positive and almost linearly increasing as a function of $-\ln(\delta s)$, and an intermittency signal is observed. Region 1, corresponding to evaporation, gives zero slope. Increasing or reducing the size of the three cuts in the respective regions does not change significantly these results. The interpretation of experimentally observed intermittency signals may, however, be problematic due to ensemble averaging effects [24], even though calculations show that impact parameter averaging only increases the absolute value of the SFM [25]. Since cut 2 may involve a large range of impact parameters, the observed intermittency signal could be an artifact of ensemble averaging and can, therefore, not be taken as a definitive proof of unusually large fluctuations in a sharply defined class of events.

In conclusion, we have analyzed fragment production in Au + Au collisions at $E = 35$ MeV/nucleon. Events were selected by requiring a total detected charge between 70 and 90 and the velocity of the largest detected fragment larger than 75% of the projectile velocity. A Campi scatter plot of these events displays two branches similar to the subcritical and overcritical branches observed in theoretical studies. The selection of events from the intersection of these two branches (which has been associated with critical events in theoretical studies) shows power-law charge distributions with an exponent of $\tau \approx 2.2$ similar to that characterizing the mass distribution near the critical point of a liquid-gas transition. These events further display an intermittent behavior similar to that expected for near-critical events. While these signatures have been associated with near-critical events, we must caution that the effects of finite experimental acceptance and event mixing with possible contributions from the decay of projectile-like fragments and the neck region are not yet sufficiently well understood to allow an unambiguous conclusion of critical behavior in the present reaction. Our work does, however, show that different regions of the nuclear phase diagram can be probed at one incident beam energy by selecting events according to different impact parameters and/or energy depositions.

One of the authors (M.B.) thanks the Physics Department of the University of Trieste for financial support and the Physics Department of the University of Bologna,

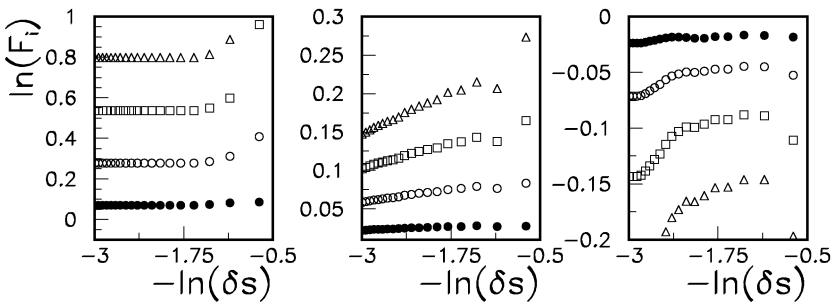

FIG. 4. Scaled factorial moments $\ln(F_i)$ versus $-\ln(\delta s)$ for the three cuts indicated in Fig. 2; the left part of the figure corresponds to cut 1, the central part to cut 2, and the right part to cut 3. Solid points represent the SFM of order $i = 2$, open circles $i = 3$, open squares $i = 4$, and open triangles $i = 5$.

where the major part of this work has been done, for warm hospitality and financial support. This work has been supported in part by funds of the Italian Ministry of University and Scientific Research. The authors would like to thank R. Bassini, C. Boiano, S. Brambilla, G. Busacchi, A. Cortesi, M. Malatesta, and R. Scardaoni for their technical assistance.

[1] J. E. Finn *et al.*, Phys. Rev. Lett. **49**, 1321 (1982); Phys. Lett. **118B**, 458 (1982); M. Mahi *et al.*, Phys. Rev. Lett. **60**, 1936 (1988).

[2] R. G. Palmer and P. W. Anderson, Phys. Rev. D **9**, 3281 (1974); W. G. Kupper, G. Wegmann, and E. R. Hilf, Ann. Phys. (N.Y.) **88**, 454 (1974); G. Sauer, H. Chandra, and U. Mosel, Nucl. Phys. **A264**, 221 (1976); D. Q. Lamb, J. M. Lattimer, C. J. Pethick, and D. G. Ravenhall, Phys. Lett. **41**, 1623 (1978); Nucl. Phys. **A360**, 459 (1981); H. Schulz, L. Münchow, G. Röpke, and M. Schmidt, Phys. Lett. **119B**, 12 (1982); Nucl. Phys. **A399**, 587 (1983); H. R. Jaqaman, A. Z. Mekjian, and L. Zamick, Phys. Rev. C **27**, 2782 (1983); **29**, 2067 (1984).

[3] M. W. Curtain, H. Toki, and D. K. Scott, Phys. Lett. **123B**, 289 (1983); A. D. Panagiotou, M. W. Curtain, H. Toki, D. K. Scott, and P. J. Siemens, Phys. Rev. Lett. **52**, 496 (1984); G. F. Bertsch and P. J. Siemens, Phys. Lett. **126B**, 9 (1983).

[4] A. L. Goodman, J. I. Kapusta, and A. Z. Mekjian, Phys. Rev. C **30**, 851 (1984); H. R. Jaqaman, Gabor Papp, and D. H. E. Gross, Nucl. Phys. **A514**, 327 (1990).

[5] J. B. Elliot, M. L. Gilkes, J. A. Hauger, A. S. Hirsch, E. Hjort, N. T. Porile, R. P. Scharenberg, B. K. Srivastava, M. L. Tincknell, and P. G. Warren, Phys. Rev. C **49**, 3185 (1994); M. L. Gilkes *et al.*, Phys. Rev. Lett. **73**, 1590 (1994).

[6] V. Latora, M. Belkacem, and A. Bonasera, Phys. Rev. Lett. **73**, 1765 (1994); M. Belkacem, V. Latora, and A. Bonasera, Phys. Rev. C **52**, 271 (1995).

[7] J. Pochodzalla *et al.*, Phys. Rev. Lett. **75**, 1040 (1995).

[8] I. Iori *et al.*, Nucl. Instrum. Methods Phys. Res., Sect. A **325**, 458 (1993).

[9] R. T. DeSouza *et al.*, Nucl. Instrum. Methods Phys. Res., Sect. A **295**, 109 (1990).

[10] D. H. E. Gross, Prog. Nucl. Phys. **30**, 155 (1993); A. S. Botvina and D. H. E. Gross, Nucl. Phys. **A592**, 257 (1995).

[11] J. Bondorf *et al.*, Nucl. Phys. **A444**, 460 (1985); J. Bondorf, A. S. Botvina, A. S. Iljinov, I. N. Mishustin, and K. Sneppen, Phys. Rep. **257**, 133 (1995).

[12] M. D'Agostino *et al.*, Phys. Rev. Lett. **75**, 4373 (1995); Phys. Lett. B (to be published).

[13] C. P. Montoya *et al.*, Phys. Rev. Lett. **73**, 3070 (1994).

[14] A. Bonasera, F. Gulminelli, and J. Molitoris, Phys. Rep. **243**, 1 (1994).

[15] M. Belkacem *et al.* (to be published).

[16] X. Campi, J. Phys. A **19**, L917 (1986); X. Campi, Phys. Lett. B **208**, 351 (1988); J. Phys. (Paris) **50**, 183 (1989).

[17] H. R. Jaqaman and D. H. E. Gross, Nucl. Phys. **A524**, 321 (1991); D. H. E. Gross, A. R. DeAngelis, H. R. Jaqaman, Pan Jicai, and R. Heck, Phys. Rev. Lett. **68**, 146 (1992); A. R. DeAngelis, D. H. E. Gross, and R. Heck, Nucl. Phys. **A537**, 606 (1992).

[18] The charge distributions shown in Fig. 3 and the SFM shown in Fig. 4 have been calculated without the heaviest fragment in each event, apart from the charge distribution of cut 1.

[19] W. Bauer *et al.*, Phys. Lett. **150B**, 53 (1985); Nucl. Phys. **A452**, 699 (1986); Phys. Rev. C **38**, 1297 (1988).

[20] M. E. Fisher, Rep. Prog. Phys. **30**, 615 (1967); in *Critical Phenomena*, Proceedings of the International School of Physics "Enrico Fermi," Course LI, edited by M. S. Green (Academic, New York, 1971); Phys. **3**, 255 (1967).

[21] A. Bialas and R. Peschanski, Nucl. Phys. **B273**, 703 (1986); **B308**, 857 (1988).

[22] M. Ploszajczak and A. Tucholski, Phys. Rev. Lett. **65**, 1539 (1990); Nucl. Phys. **A523**, 651 (1991).

[23] X. Campi and H. Krivine, Nucl. Phys. **A589**, 505 (1995).

[24] L. Phair *et al.*, Phys. Lett. B **291**, 7 (1992).

[25] V. Latora, A. Del Zoppo, and A. Bonasera, Nucl. Phys. **A572**, 477 (1994).